Applied Surface Science 487 (2019) 510–518

Contents lists available at ScienceDirect

Applied Surface Science

journal homepage: www.elsevier.com/locate/apsusc

Full length article

The effect of oxygen coverages on hydrogenation of Mg (0001) surface

Xiaowei Chen[a,*], Weidong Zou[c], Qiubao Lin[a], Renquan Li[a], Guanglin Xia[b], Xuebin Yu[b,*]

[a] Department of Physics, School of Science, Jimei University, Xiamen 361021, China
[b] Department of Materials Science, Fudan University, Shanghai 200433, China
[c] College of Physics and Electromechanical Engineering, Longyan University, Fujian 364012, China

ARTICLE INFO

Keywords:
Hydrogen storage
Surface
Oxide
Density functional theory

ABSTRACT

The H_2 dissociation and subsequent atomic H diffusion on the oxide Mg(0001) surface have been investigated using density functional theory calculations. Our calculation indicates that at low oxygen coverages the H_2 dissociation is the rate-limiting step for surface hydrogenation. The increase of oxygen coverages from 0 to 1/4 monolayer results in decreased H_2 dissociation energy barriers from 0.93 to 0.76 eV, indicating that partial oxidized Mg(0001) surface facilitates hydrogenation. This can attributed to the enhancement of H binding strength on the oxidized Mg surface. However, the atomic H diffusion energy barriers increase with increasing H binding strength on the surface. At high oxygen coverage (1 monolayer) the diffusion of H atom from surface to subsurface is the rate-limiting step for the hydrogenation. The H atom diffusion pathways are blocked by surrounding O^{2-} anions, hence H atom needs to overcome a significantly high energy barrier of 2.38 eV to diffuse from 1 monolayer oxide surface to subsurface. This indicates that high oxygen coverages would impede the surface hydrogenation.

1. Introduction

Metal hydrides with high gravimetric and volumetric densities of hydrogen have received great attention as solid-state hydrogen storage media in the past few decades [1–6]. In particularly, magnesium hydride with a volumetric capacity of 110 g H_2/L and gravimetric capacity of 7.6 wt%, is an attractive candidate as hydrogen storage material [7–9]. However, the slow hydrogen absorption kinetics and high dehydrogenation temperature limit its practical use. The slow rate of hydrogenation of Mg can be attributed to surface oxidization, poor dissociative chemisorption of H_2 and low hydrogen diffusion constant [9–11]. Reducing Mg particle size [12–18], reducing the thicknesses of Mg with the formation of thin film [19–22], ball milled Mg with different types of transition metal and their oxides [23–26], and using catalyst [27–30] are effective approaches to improve the hydrogenation kinetics of Mg.

The formation of MgO with rock-salt structure would prevents H_2 molecules to dissociate on the surface, and impedes H atoms to penetrate from the surface to bulk [31,32]. Recent studies show that polymer poly (methyl methacrylate) (PMMA) or reduced graphene oxide (rGO) encapsulated Mg nanoparticles exhibits high-capacity hydrogen storage and rapid hydrogen absorption/desorption kinetics [15,16]. Although a small fraction of oxidative state on the rGO encapsulated Mg nanoparticles were detected [15], the oxidation layer does not have an impact on the hydrogen storage properties of the nanoparticles [15]. Since the gas-selective rGO sheets can protect Mg nanoparticles from oxygen and moisture, the formation of magnesium oxide with rock-salt structure is not necessarily. It has been reported that magnesium can experience complex reconstructions without formation of rock-salt MgO at partial coverages of oxygen [33,34]. The H_2 dissociation and subsequent atomic H diffusion mechanism on the partial oxidized Mg surface may be different from that of rock-salt MgO surface. It raises the question that whether a limited amount of oxygen on the Mg surface would prevent the H_2 dissociation and subsequent H atom diffusion process.

So far, some theoretical works have been performed to understand the dissociation of H_2 and diffusion of H atoms on the clean and transition metals doped Mg surface [11,35–39]. For instances, it has been reported that H atom preferably adsorbs on the FCC sites of Mg(0001) surface, and H atom diffuses from surface to subsurface through the FCC-channels [11]; Pozzo et al. have proposed that doping transition metal with strong metal-H binding strength facilitates H_2 dissociation on the Mg(0001) surface, meanwhile impedes H atom diffusion into the subsurface [36]. But the effect of oxygen coverages on hydrogenation of Mg is still not well understood. In order to gain deep insights into the mechanism of Mg surface hydrogenation associated with oxygen

* Corresponding authors.
E-mail addresses: chenxiaowei@jmu.edu.cn (X. Chen), yuxuebin@fudan.edu.cn (X. Yu).

https://doi.org/10.1016/j.apsusc.2019.05.021
Received 29 December 2018; Received in revised form 5 April 2019; Accepted 3 May 2019
Available online 04 May 2019
0169-4332/

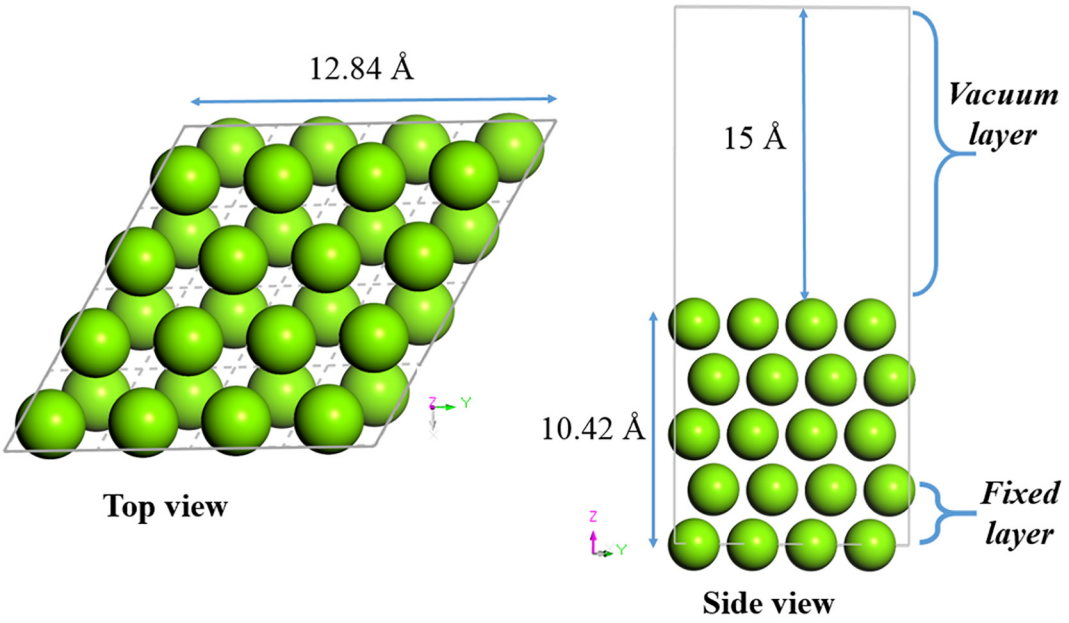

Fig. 1. Top view and side view of (4 × 4) Mg (0001) surface. The dash line indicates the unit cell of Mg(0001) surface.

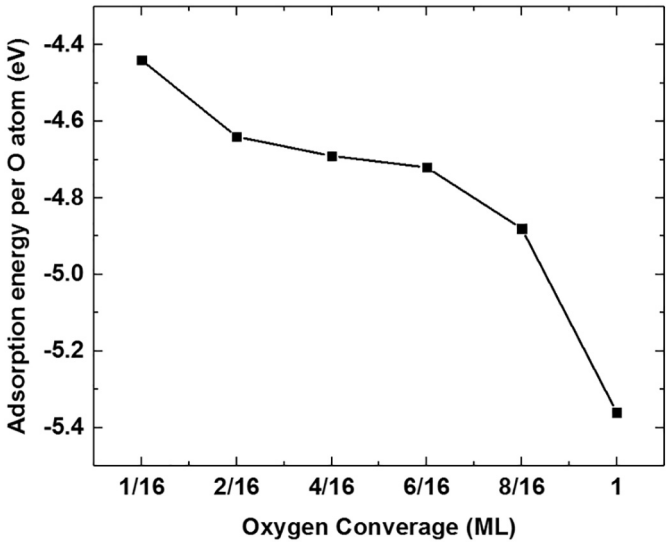

Fig. 2. The adsorption energy of O atoms on the Mg(0001) surface.

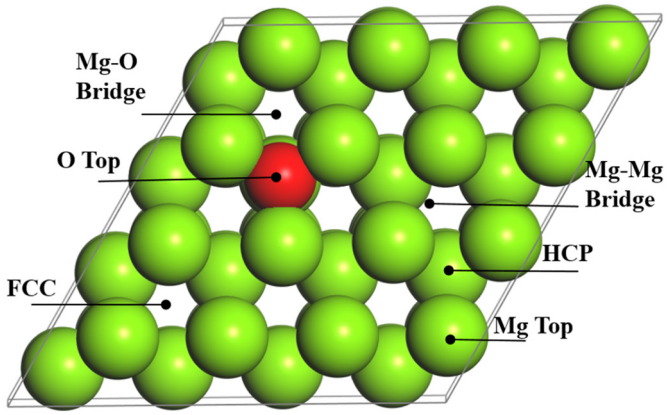

Fig. 3. Sketch of the H atom adsorption sites at oxidized Mg(0001) surface. The green and red balls represent the Mg and O atoms, respectively.

Table 1
The H atom binding energies on the clean and oxidized Mg(0001) surface.

Oxygen coverage (ML)	0	1/16	1/8	1/4	1/2	1
H atom binding energy (eV)	−0.06	−0.12	−0.20	−0.26	−0.55	−0.60

coverages, we examined the H_2 dissociation and H atom diffusion on the oxide Mg(0001) surface and studied the effect of oxygen coverages on the overall hydrogen uptake process.

2. Computational method

The geometric structures were optimized by DFT calculation as implemented in MedeA@VASP code [40]. The projector-augmented wave (PAW) approach was used to describe the electron-ion interactions [41]. The plane wave with kinetic energy cutoff of 400 eV was used. The generalized gradient approximation (GGA) of Perdew-Burke-Ernzerhof (PBE) was adopted to describe the exchange and correlation of electronics [42,43]. The Brillouin zone was sampled by Monkhorst–Pack *k*-point meshes [44] with mesh point spacing < 0.03 per Å. The H_2 dissociation and H diffusion barriers were estimated by using the climbing image nudged elastic band (CI-NEB) method [45].

Previous DFT calculation indicates that the Mg(0001) surface has substantially low surface energy, therefore we used this surface for all subsequent calculations in this paper [11,40]. The bulk magnesium with lattice constants of $a = b = 3.21$ Å, c = 5.21, $\alpha = \beta = 90^o$, $\gamma = 120^o$ and space group of *P63/mmc* was used to setup the Mg (0001) surface. As shown in Fig. 1, the Mg (0001) surface was modeled by using a (4 × 4) surface unit cell with five layers slab repeated periodically. The created Mg (0001) surface has lattice constants of $a = b = 12.84$ Å and $\alpha = \beta = 90^o$, $\gamma = 120^o$. An additional 15 Å vacuum layer was placed between the slabs to ensure separation, resulting in a supercell of 25.42 Å in the *z*-direction. The structure was optimized by allowing the first three atomic layers to relax, while the bottom two layers and lattice constants were fixed. The residual force was minimized to 0.02 eV/Å for the geometry optimization. Spin-polarization was tested and found to have a negligible influence on the binding energies, energy barriers, and optimized structures. Hence, spin-polarization was not included in the calculated results.

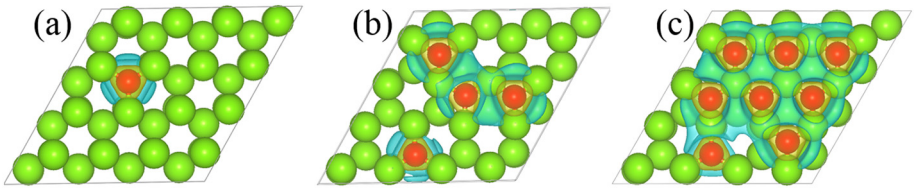

Fig. 4. Charge density difference plots for (a) 1/16 ML, (b) 1/4 ML, and (c) 1/2 ML oxidized Mg(0001) surface. The color scheme is blue for positive charge density and yellow for negative charge density. Isosurface charge density is taken to be 0.0032.

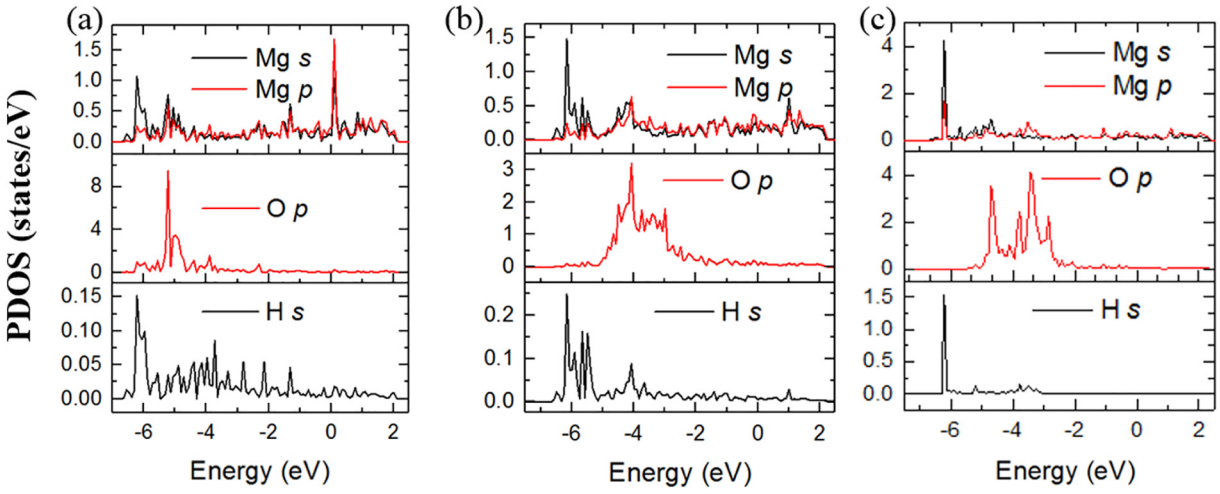

Fig. 5. Projected density of states (PDOS)of H, O and Mg for the (a) 1/16 ML, (b) 1/8 ML and (c) 1/2 ML oxidized Mg(0001) surface.

As one closed packed Mg (0001) layer contains 16 Mg atoms, one monolayer coverage (ML) is defined as 16 oxygen atoms adsorb on the (4 × 4) surface. Hence, one O atom adsorbs on the surface corresponds to a coverage of 1/16 ML of oxygen.

The O adsorption energy was defined as:

$$\Delta E_O = [E(Mg + O) - E(Mg) - E_{O2} \times n/2]/n$$

where $E(Mg + O)$ is the total energy of oxidized Mg (0001) surface, E_{O2} represents the energy of the isolated O_2 molecule, and $E(Mg)$ is the total energy of clean Mg (0001) surface, n is the number of adsorption O atom.

The H atom binding energy was defined as:

$$\Delta E_H = E(Mg + H) - E(Mg) - E_{H2} \times 1/2$$

where $E(Mg)$ is the total energy of Mg (0001) surface, E_{H2} represents the energy of the isolated H_2 molecule, and $E(Mg + H)$ is the total energy of Mg (0001) surface with the adsorption of H atom.

A positive value of ΔE indicates that the adsorption of O or H atom is an endothermic process, and the negative values of ΔE denote the adsorption that is more stable than the corresponding clean surface and gas phase.

3. Results

3.1. Adsorption of atomic H on the oxidized Mg(0001) surface

We begin this part of the study by examining the adsorption of O atoms on the Mg(0001) surface. Schröder et al. compared several oxygen adsorption sites on the Mg(0001) surface and found that the O is incorporated below the topmost Mg layer in tetrahedral sites for oxygen coverages lower than 1 ML [33]. Following this work, the oxygen adsorption energies on different oxygen coverages Mg(0001) surface were calculated and presented in Fig. 2. The adsorption of O atoms on the Mg (0001) surface are exothermic processes and the average oxygen adsorption energies decrease with increasing oxygen coverage, in good agreement with previous work [33].

It has been reported that the hydrogen atom prefers to adsorb on the FCC sites of clean Mg(0001) surface [11,35–37]. We further investigated the atomic H adsorbs on the FCC, HCP, Mg—Mg bridge, O top and Mg—O bridge sites of oxidized Mg(0001) surface (as shown in Fig. 3). We found that the H adsorbs on the FCC, HCP and Mg—Mg bridge sites of oxidation Mg(0001) surface are exothermic processes, while the adsorption of H on O top sites or Mg—O bridge sites with formation of O—H bonds are thermodynamically unstable. In addition, H atom adsorbs on the FCC sites with the lowest negative binding energy, similar to that on the clean surface [35–37].

The calculated H binding energies on the oxidized Mg(0001) surface were summarized in Table 1. The hydrogen binding energy on clean Mg (0001) surface is −0.06 eV, in good agreement with previous theoretical work [35]. Interestingly, the hydrogen binding energies decrease with increasing oxygen coverage. Since the negative value of binding energy indicates that the adsorption of H atom on the Mg surface is exothermic process, the lower negative value of binding energy suggests the stronger H binding strength on the surface.

It has been reported that the charge transfer of Mg atoms upon the lattice expansion results in the enhancement of the Mg—H bonding [46]. The oxidation would modify the electronic structure of Mg surface and consequently case charge transfer from Mg to O, which might be a clue to clarify the binding strength between H atom and the oxidized surface. To understand the charge transfer caused by O adsorption, the charge density difference (CDD) was investigated.

The CDD of O adsorption on Mg surface is defined as

$$\Delta\rho(\mathrm{Mg + O}) = \rho(\mathrm{Mg + O}) - \rho(\mathrm{Mg}) - \rho(\mathrm{O})$$

where ρ(Mg + O) is the total charge density distribution of the oxidized surface, ρ(Mg) and ρ(O) are the charge density distribution of the isolated Mg surface and O atoms with the same atomic positions as the oxidized surface, respectively.

As indicated by the contour plots in Fig. 4(a)–(c), the adsorption of O on the surface results in charge transfer between O atom and the neighboring surface Mg atoms. The O atom absorbs extra electrons to form the negative charge center (in yellow). The Mg surface layer loses electrons to form the positive charge region on Mg—Mg bridge sites (in blue). The charge transfer from Mg to O on the oxide surface lead to

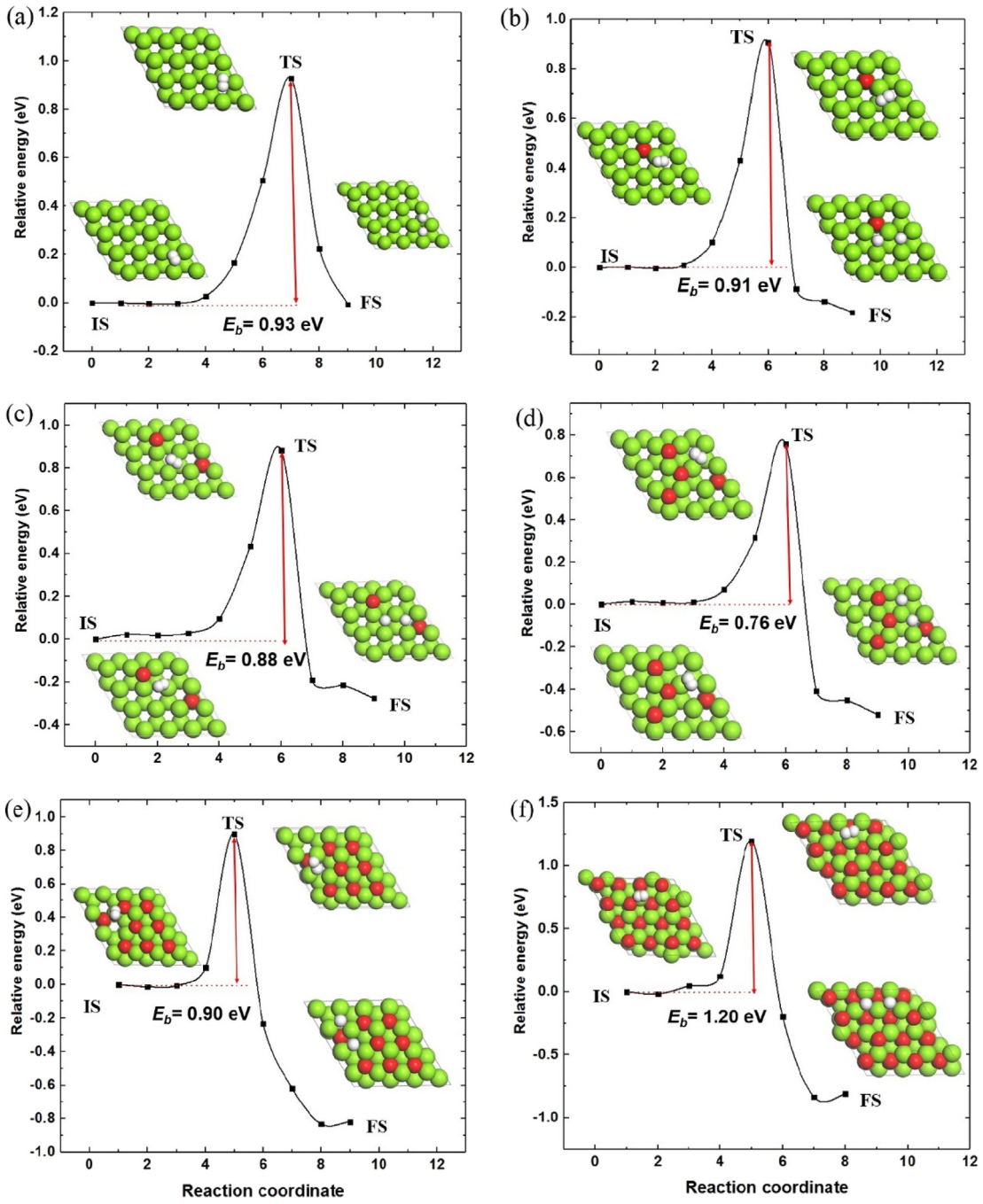

Fig. 6. Dissociation pathway for H_2 molecule on the clean Mg(0001) surface (a), 1/16 ML (b), 1/8 ML (c), 1/4 ML (d), 1/2 ML (e), 1 ML (f) oxidized Mg(0001) surface.

Table 2
Summarized H_2 energy barriers and atom distances at the transition state of H_2 dissociation.

Oxygen coverage (ML)	H_2 Dissociation barrier (eV)	Atom distances at the transition state (Å)		
		H-H	Mg-H	O-H
0	0.93	1.06	2.05	–
1/16	0.91	1.06	2.03	3.49
1/8	0.88	0.99	2.09	3.52
1/4	0.76	0.99	2.08	3.39
1/2	0.90	1.18	1.90	2.65
1	1.20	1.06	2.04	2.53

increased electric field around Mg.

We further explore the projected density of states (PDOS) of H atom adsorbs on the oxide surface to investigate the orbital interaction mechanism in the H adsorption. As indicates by Fig. 5, the O *p* orbital hybridizes with the s and *p* orbitals of its neighboring Mg atoms. Hence, the bonding interaction of O atoms with Mg surface is dominated by the *s*(O)-*s*(Mg) and *p*(O)-*s*(Mg) orbital hybridization. The H *s* orbital mainly hybridizes with the Mg *s* orbital and a little Mg *p* orbital, similar to that of H atom adsorbs on the clean Mg(0001) surface [46]. Interestingly, the intensity of H *s* peak around −6.2 eV increases with increased oxygen coverage, which responses to the increase of Mg—H binding strength.

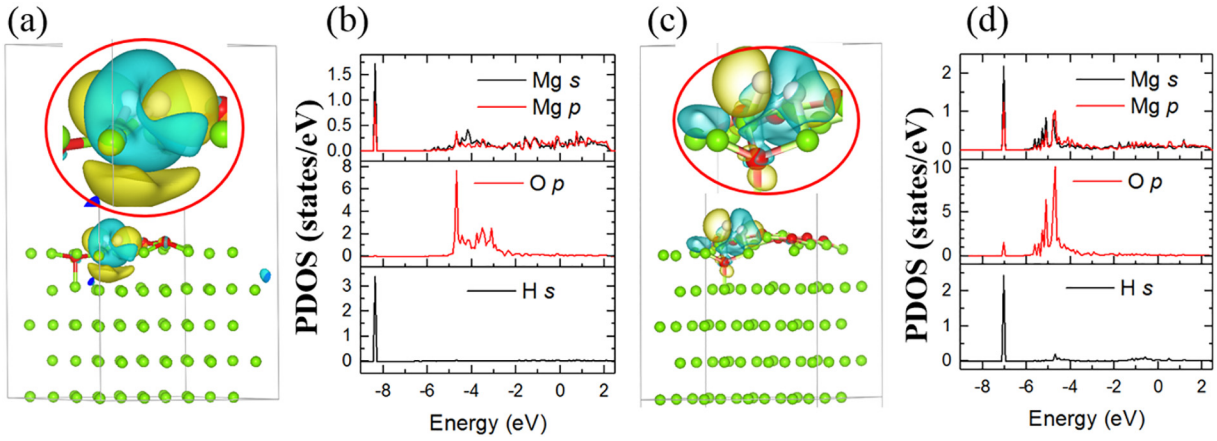

Fig. 7. Charge density difference and projected density of states (PDOS)for the transition state of H_2 dissociated on 1/4 ML(a-b) and 1/2 ML (c-d) oxide Mg(0001) surface. The color scheme in (a) and (c) is blue for positive charge density and yellow for negative charge density. Iso-surface charge density is taken to be 0.0006 electrons/Å^3.

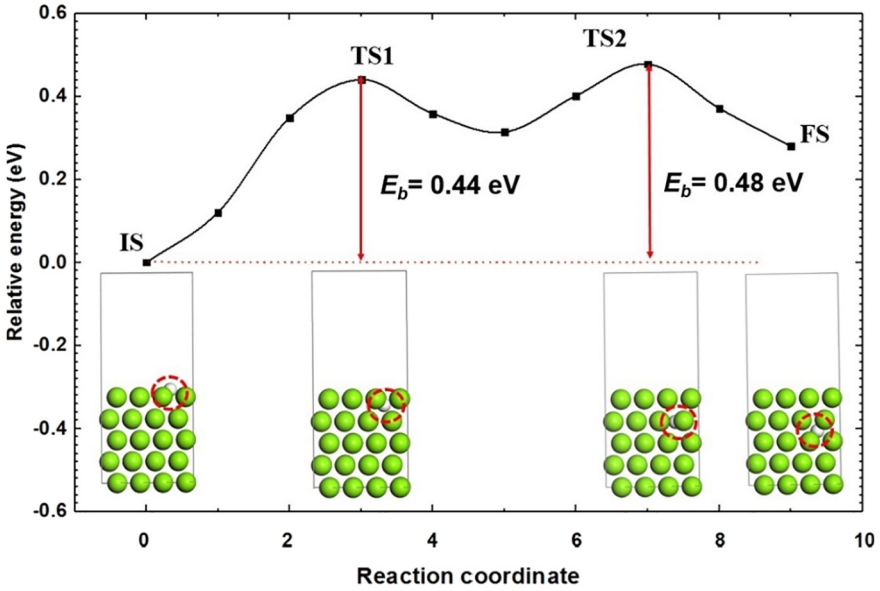

Fig. 8. Diffusion pathway for hydrogen atom on the clean Mg(0001) surface.

3.2. Dissociation of H_2 on the oxidized Mg(0001) surface

As discussed above, the H atom prefers to adsorb on the FCC sites of the clean and oxidized Mg(0001) surface. Hence, the dissociation of H_2 on the clean and oxidized Mg (0001) surface can be considered as two H atoms occupying the neighboring FCC sites. As presented in Fig. 6(a), our calculation shows an energy barrier of 0.93 eV for H_2 dissociates over the FCC sites of Mg(0001) surface, in good agreement with previous reports [36,37]. As shown in Fig. 6(b), the calculated energy barrier for H_2 dissociates on the 1/16 ML coverage Mg (0001) surface is 0.91 eV, which is 0.02 eV lower than that of the clean surface. Fig. 6(c) and (d) shows that the energy barriers for H_2 dissociates on 1/8 and 1/4 ML oxide surface are 0.88 and 0.76 eV, respectively. The H_2 dissociation energy barriers decrease with increasing oxygen coverages from 0 to 1/4 ML. However, further increases the oxygen coverages to 1/2 ML and 1 ML results in increased H_2 dissociation energy barriers. Particularly, with the formation of 1 ML oxide Mg (0001) surface, the H_2 molecule needs to overcome an energy barrier of 1.20 eV to dissociate on the surface, which is 0.27 eV higher in energy barrier than that of the clean surface.

Our above calculation indicates that the oxidized Mg surface is not always prevented H_2 molecule dissociation. Low oxygen coverages ($\leq$1/4 ML) facilitate H_2 dissociates on the surface, but high oxygen coverages (1/2 and 1 ML) result in relatively high H_2 dissociation energy barriers.

As presented in Fig. 6 and Table 2, the transition state of H_2 dissociated on the clean and oxidized Mg(0001) surface shows some similar features. The H_2 located at Mg—Mg bridge sites with H—H distances range from 0.99 to 1.18 Å, indicating that the covalent bonding of H—H dimer is still preserved at the transition state. The Mg—H distances range from 1.90 to 2.08 Å, slightly longer than Mg—H bond length of 1.94 Å in bulk MgH_2.

The CDD of the transition state of H_2 dissociated on the oxidized Mg surface is calculated using the following equation.

$$\Delta\rho = \rho(\mathrm{Mg + O + H}) - \rho(\mathrm{Mg + O}) - \rho(\mathrm{H})$$

where ρ(Mg + O + H) is the total charge density distribution of transition state of H_2 dissociated on the oxidized Mg surface, ρ(Mg + O) and ρ(H) are the charge density distribution of the oxidized Mg surface and H—H dimer at the transition state, respectively.

For the 1/4 ML oxide surface, Fig. 7(a) shows that the covalent bonding of H—H dimer is still preserved at the transition state. Meanwhile, the charge density distribution between H—H dimer and its neighboring Mg atoms indicates partial Mg—H ionic bonding character.

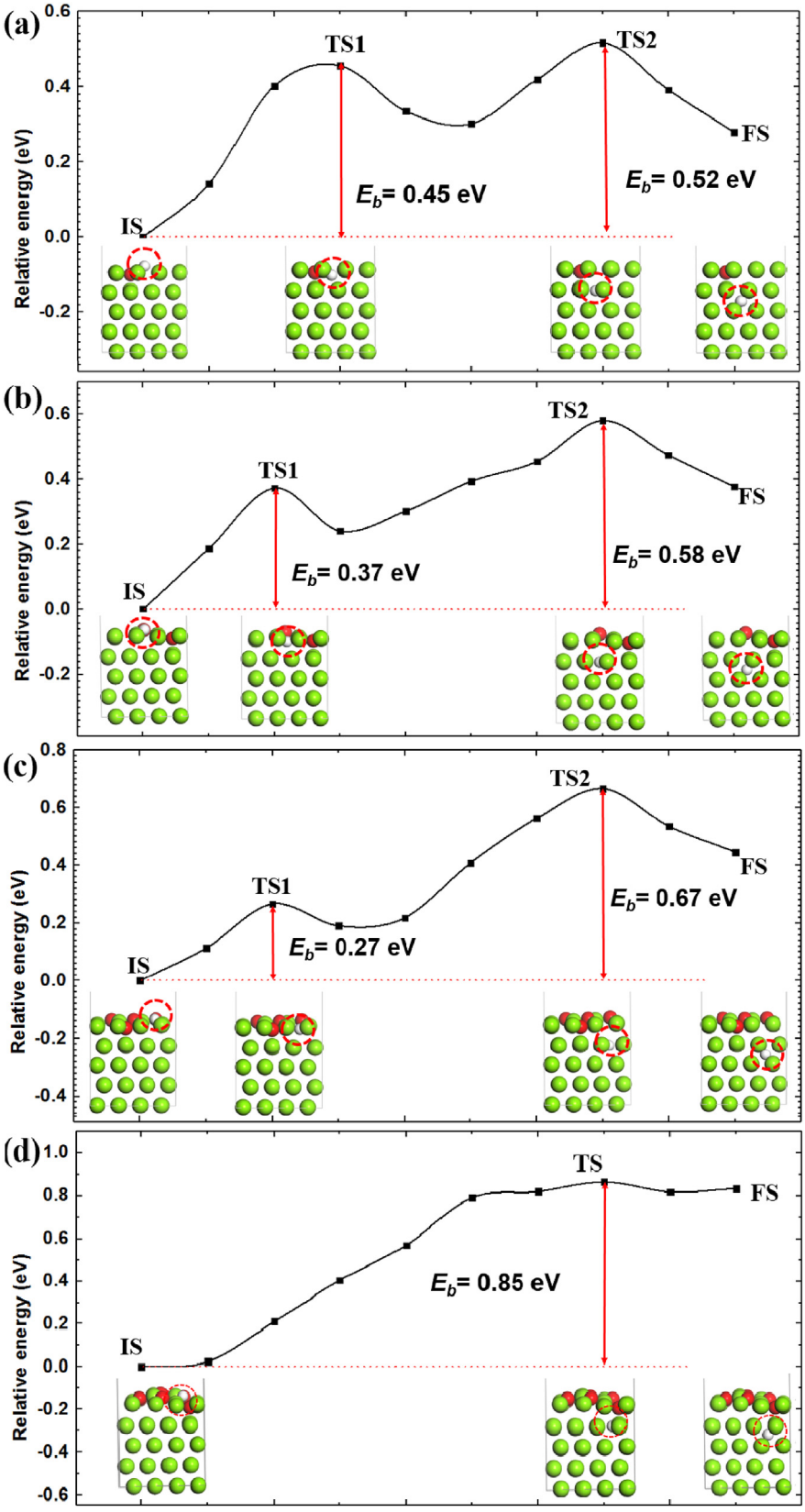

Fig. 9. Diffusion pathways for hydrogen atom on the 1/16 ML (a), 1/8 ML (b) and 1/4 ML (c) oxidized Mg(0001) surface.

For low oxygen coverages (≤1/4 ML), the H binding strength on the surface increases with increasing oxygen coverage. The distance between O and H range from 3.39 to 3.52 Å, which are longer than the sum of their van der Waals radii. As shown in Fig. 7(a), the repulsive Coulomb interaction between H−H dimer and O^{2-} is screened by surrounding Mg atoms. In addition, the Mg atoms transfer electrons to fill the H−H anti-bonding orbital. As illustrated in Fig. 7(b), for the 1/4 ML oxide Mg(0001) surface, the calculated PDOS shows sharp peaks of

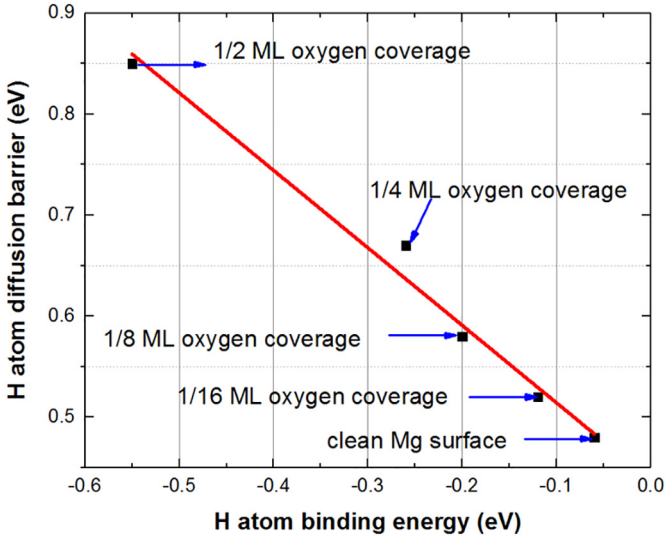

Fig. 10. The correlation between the H atom diffusion energy barriers and H atom binding energies on clean and oxidized Mg(0001) Surface.

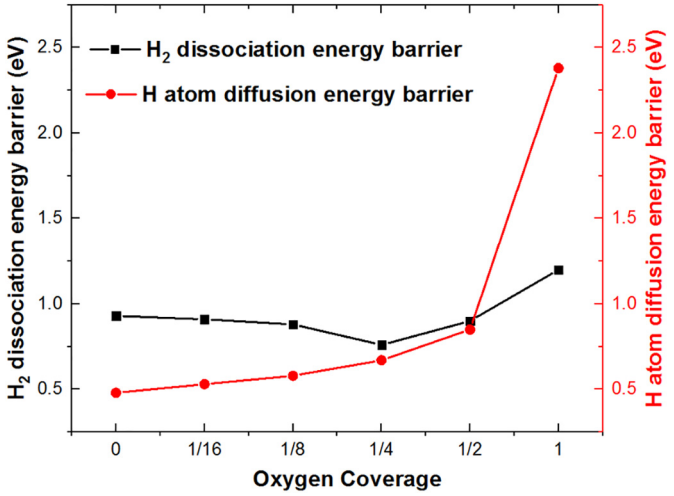

Fig. 12. Summarized hydrogen molecule dissociation energy barriers and H atom diffusion energy barriers for different coverages of oxygen on the Mg (0001) surface.

H s, Mg s and Mg *p* located at −8.2 eV, indicating that the s(H)-s(Mg) and s(H)-*p*(Mg) orbital hybridization are dominant in the bonding interaction for the H_2 molecular dissociation at the transition state. For high oxygen coverages (1/2 and 1 ML), as shown in Table 2, the distances between O and H reduce to 2.65 and 2.53 Å, respectively. These distances are slightly shorter than the sum of their van der Waals radii. As illustrated in Fig. 7(c), for the 1/2 ML oxide surface, at the transition state of H_2 dissociation, the H−H dimer is surrounded by O^{2-} and the repulsive Coulomb interaction between H−H dimer and O^{2-} increased. Compared to that of 1/4 ML oxide Mg(0001) surface, less electrons were transfer from Mg to the H−H dimer for the 1/2 ML oxide surface. The PDOS results (Fig. 7(b) and (d)) show that with oxygen coverage increases from 1/4 to 1/2 ML, the sharp peaks of H s, Mg s, Mg *p* shift from −8.3 to −7 eV, which presumably leads to higher energy barrier for H_2 dissociation.

3.3. Diffusion of hydrogen atom on the oxidized Mg(0001) surface

The previous report suggests that the diffusion barrier of H atom from the surface to subsurface is significantly lower than the barrier of H_2 dissociates on the Mg surface. Thus the dissociation of H_2 is the rate-limiting step for the ab−/de-sorption of hydrogen [11]. Although our above calculation indicates that low coverages of oxygen on Mg surface would facilitate the dissociation of H_2, the oxidized Mg surface may block the pathways for H atom penetrates from the surface to subsurface. Therefore the diffusion of H atom from oxidized Mg surface to subsurface was investigated. For comparison, the diffusion of H atom on clean Mg (0001) surface was also examined.

The hydrogen atoms preferably diffuse from clean Mg (0001) surface to subsurface through the FCC-channel as reported in previous work [11,38,39]. Therefore, similar hydrogen atom diffusion pathway on clean Mg (0001) surface was calculated. As presented in Fig. 8, our calculation shows two transition states with the energy barriers of 0.44 and 0.48 eV. The first transition state (TS1 in Fig. 8) corresponds to the process that the hydrogen atom diffuses from first to second Mg layer. The second transition state (TS2 in Fig. 8) corresponds to the process that the hydrogen atom diffuses from second to third Mg layer. The effective energy barrier for hydrogen atom diffuses from clean Mg

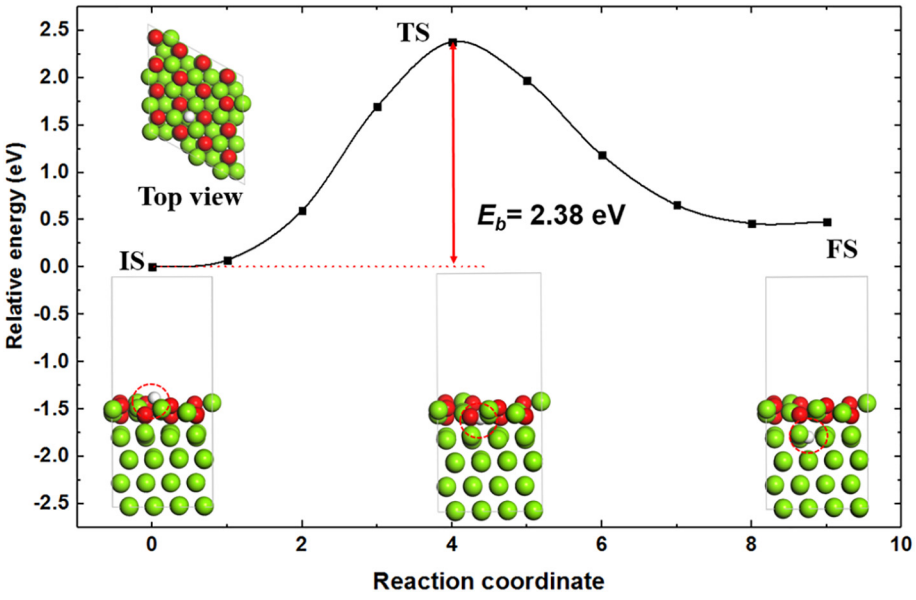

Fig. 11. Diffusion of the hydrogen atom on the 1 ML oxidized Mg(0001) surface.

(0001) surface to third Mg layer is 0.48 eV, in consistent with the previous report [39].

We further calculated the energy barriers for hydrogen atom diffuses from oxidized Mg (0001) surface to subsurface, the calculation results were summarized in Fig. 9. For oxygen coverages lower than 1/2 ML, two transition states were found for hydrogen diffusion, similar to that on the clean Mg surface. The energy barriers for the first transition state (TS1 in Fig. 9) decrease from 0.45 to 0.27 eV with the increasing oxygen coverage from 0 to 1/4 ML. The adsorption of oxygen atoms on the surface results in movement of surrounding Mg atoms toward O atoms. The Mg—Mg distances slightly increase from 3.209 to 3.254 Å with the oxygen coverage increases from 0 to 1/4 ML. Hence, the lower barriers for hydrogen atom diffuses from first to second Mg layer may be attributed to the larger Mg—Mg distances, which results in more space for the hydrogen atom to diffuse through. The energy barriers for the hydrogen atom diffuses from second to third Mg layer (TS2 in Fig. 9(a)–(c) and TS in Fig. 9(d)) increase gradually from 0.48 to 0.85 eV with increasing oxygen coverages from 0 to 1/2 ML. Since energy barriers of H diffuses from second Mg layer to third layer are higher than that of H diffuses from first Mg layer to second layer, the effective energy barrier E_b of H atom diffuses from surface to third Mg layer was defined as $E_b = E_{TS} - E_{IS}$, where E_{IS} is the total energy of the initial state (IS), E_{TS} is the total energy of transition state TS2 in Fig. 9(a)–(c) and TS in Fig. 9(d). This indicates that H atom diffuses from the surface to third Mg layer needs to overcome energy barriers of 0.52, 0.58, 0.67 and 0.85 eV for 1/16 ML, 1/8 ML, 1/4 and 1/2 ML oxide surface, respectively.

Based on the pathways calculated from the Figs. 8 and 9, the effective energy barriers of H diffusion as the function of H binding energies were plotted in Fig. 10. The H diffusion energy barriers linearly increase as the H binding energies decrease, indicating that the stronger binding of H atom on the surface results in higher H diffusion energy barriers. As shown in Figs. 8 and 9, the H diffusion follows the similar pathway for clean and oxide surface. The stronger H binding energy means lower total energy of initial state, which lead to higher H atom diffusion energy barrier.

In the case of 1 ML oxide surface, as shown in Fig. 11, all the first layer Mg atoms coordinate with oxygen atoms and the FCC-channels for hydrogen diffusion are blocked. The calculated hydrogen diffusion barrier is as high as 2.38 eV, suggesting that the high oxygen coverage (1 ML) would impede the H atom diffuses into the subsurface. The previous study also demonstrated that oxidation of the Mg surface with the formation of the MgO layer leads to prohibitively high energy barrier for hydrogen diffusion [22].

4. Discussion

The energy barriers of H_2 dissociation and energy barrier of H atom diffuses from surface to subsurface on different coverages of oxygen on the Mg (0001) surface were summarized in Fig. 12. Our calculation indicates that there is a correlation between the H_2 dissociation barriers and oxygen coverages. The hydrogen binding strength on the surface increases with increasing oxygen coverages, which lead to decrease in H_2 dissociation barriers on low oxygen coverages ($\leq$1/4 ML) surface. Therefore, in contrast to conventional wisdom that the oxidized Mg surface would block the dissociation of H_2 molecules, our calculated indicates that partial oxidation of Mg surface with low oxygen coverages ($\leq$1/4 ML) would facilitate H_2 molecules dissociation on the surface. However, further increases the oxygen coverages from 1/4 to 1 ML results in increased repulsive Coulomb interaction between O^{2-} and H—H dimer, which responsible for the increased H_2 dissociation barriers from 0.76 to 1.20 eV. Hence, high oxygen coverages would block H_2 molecule dissociates on Mg (0001) surface.

On the other hand, the increases of H binding strength on the surface results in increased energy barriers for hydrogen atom diffuses from first to third Mg layer. In the case of 1 ML oxide surface, the pathways for the hydrogen diffusion are blocked by O^{2-}, which results in significantly high hydrogen diffusion energy barrier.

The rate-limiting step for the surface hydrogenation is the one with the largest energy barrier between H_2 dissociation and H atom diffusion. It has been reported that the dissociation of H_2 is the rate-limiting step for the hydrogenation of Mg [11]. As shown in Fig. 12, for oxygen coverages range from 0 to 1/4 ML, the energy barriers of hydrogen dissociation are higher than the energy barriers of hydrogen diffusion, which indicates that the H_2 dissociation is still the rate-limiting step for the hydrogenation of Mg. The energy barriers of the rate-limiting step decrease from 0.93 to 0.76 eV with increasing oxygen coverages from 0 to 1/4 ML, indicating that partial oxidation of Mg(0001) surface facilitates surface hydrogenation. The energy barrier of hydrogen dissociation and diffusion are comparable in the 1/2 ML oxide surface. In the case of 1 ML oxygen coverage surface, the energy barrier of hydrogen diffusion is significantly higher than that of hydrogen dissociation. Therefore, the diffusion of hydrogen from the surface to subsurface is the rate-limiting step for the hydrogenation of the 1 ML oxide surface.

5. Conclusion

Using DFT calculations, we explored the H_2 dissociation and atomic H diffusion mechanism on the oxygen coverages of Mg(0001) surface. Our calculation shows that the increase of oxygen coverages lead to increased H binding strength on the surface, which responsible for the decrease in H_2 molecule dissociation barriers (oxygen coverages range from 0 to 1/4 ML). However, high oxygen coverages (1/2 ML and 1 ML) results in relatively strong Coulomb repulsion between H—H dimer and O^{2-}, which lead to high energy barriers of H_2 dissociation. Besides, at oxygen coverages range from 0 to 1/2 ML, the hydrogen atom diffusion energy barriers linearly increase with increasing H binding strength on the surface. In the case of 1 ML oxide surface, the H atom diffusion pathway is blocked by surrounding O^{2-} anions, which results in high energy barrier for hydrogen diffusion.

At low oxygen coverages, the H_2 dissociation is the rate-limiting step for the Mg(0001) surface hydrogenation and the corresponding energy barriers decrease from 0.93 to 0.76 eV with increasing oxygen coverages from 0 to 1/4 ML. This indicates that partial oxidation of Mg (0001) surface with low oxygen coverages can facilitate hydrogenation. At the high oxygen coverage, penetration of hydrogen atom from surface to subsurface is the rate-limiting step for the hydrogenation. The significantly high energy barrier of 2.38 eV would impede H atom diffuses from 1 ML oxide surface into the subsurface. We hope that our calculation provides useful insights for understanding the effect of oxygen coverages on the hydrogenation of Mg.

Conflicts of interest

There are no conflicts to declare.

Acknowledgements

This work is supported by the National Natural Science Foundation of China (51601068, 51625102, 51471053), Natural Science Foundation of Fujian Province (2016J05129).

References

[1] W. Grochala, P.P. Edwards, Thermal decomposition of the non-interstitial hydrides for the storage and production of hydrogen, Chem. Rev. 104 (2004) 1283–1316.
[2] B. Sakintuna, F. Lamari-Darkrim, M. Hirscher, Metal hydride materials for solid hydrogen storage: a review, Int. J. Hydrog. Energy 32 (2007) 1121–1140.
[3] U. Eberle, M. Felderhoff, F. Schuth, Chemical and physical solutions for hydrogen storage, Angew. Chem. Int. Ed. 48 (2009) 6608–6630.
[4] S. Qiu, H. Chu, Y. Zou, C. Xiang, F. Xu, L. Sun, Light metal borohydrides/amides combined hydrogen storage systems: composition, structure and properties, J. Mater. Chem. A 5 (2017) 25112–25130.
[5] L. Yongfeng, Y. Yaxiong, G. Mingxia, P. Hongge, Tailoring thermodynamics and

kinetics for hydrogen storage in complex hydrides towards applications, Chem. Rec. 16 (2016) 189–204.
[6] Y. Liu, H. Pan, M. Gao, Q. Wang, Advanced hydrogen storage alloys for Ni/MH rechargeable batteries, J. Mater. Chem. 21 (2011) 4743–4755.
[7] M. Dornheim, S. Doppiu, G. Barkhordarian, U. Boesenberg, T. Klassen, O. Gutfleisch, R. Bormann, Hydrogen storage in magnesium-based hydrides and hydride composites, Scr. Mater 56 (2007) 841–846.
[8] K.-F. Aguey-Zinsou, J.-R. Ares-Fernandez, Hydrogen in magnesium: new perspectives toward functional stores, Energy Environ. Sci. 3 (2010) 526–543.
[9] I.P. Jain, C. Lal, A. Jain, Hydrogen storage in Mg: a most promising material, Int. J. Hydrog. Energy 35 (2010) 5133–5144.
[10] A. Zaluska, L. Zaluski, J.O. Ström–Olsen, Nanocrystalline magnesium for hydrogen storage, J. Alloys Compd. 288 (1999) 217–225.
[11] T. Vegge, Locating the rate-limiting step for the interaction of hydrogen with Mg (0001) using density-functional theory calculations and rate theory, Phys. Rev. B 70 (2004) 035412.
[12] X. Yu, Z. Tang, D. Sun, L. Ouyang, M. Zhu, Recent advances and remaining challenges of nanostructured materials for hydrogen storage applications, Prog. Mater. Sci. 88 (2017) 1–48.
[13] T.K. Nielsen, F. Besenbacher, T.R. Jensen, Nanoconfined hydrides for energy storage, Nanoscale 3 (2011) 2086–2098.
[14] T.K. Nielsen, K. Manickam, M. Hirscher, F. Besenbacher, T.R. Jensen, Confinement of MgH_2 nanoclusters within nanoporous aerogel scaffold materials, ACS Nano 3 (2009) 3521–3528.
[15] E.S. Cho, A.M. Ruminski, S. Aloni, Y. Liu, J. Guo, J.J. Urban, Graphene oxide/metal nanocrystal multilaminates as the atomic limit for safe and selective hydrogen storage, Nat. Commun. 7 (2016) 10804.
[16] K.-J. Jeon, H.R. Moon, A.M. Ruminski, B. Jiang, C. Kisielowski, R. Bardhan, J.J. Urban, Air-stable magnesium nanocomposites provide rapid and high-capacity hydrogen storage without using heavy-metal catalysts, Nat. Mater. 10 (2011) 286–290.
[17] D.W. Lim, J.W. Yoon, K.Y. Ryu, M.P. Suh, Magnesium nanocrystals embedded in a metal–organic framework: hybrid hydrogen storage with synergistic effect on Physi- and chemisorption, Angew. Chem. 124 (2012) 9952–9955.
[18] H. Shao, G. Xin, J. Zheng, X. Li, E. Akiba, Nanotechnology in Mg-based materials for hydrogen storage, Nano Energy 1 (2012) 590–601.
[19] A. Baldi, M. Gonzalez-Silveira, V. Palmisano, B. Dam, R. Griessen, Destabilization of the Mg-H system through elastic constraints, Phys. Rev. Lett. 102 (2009) 226102.
[20] J. Qu, Y. Wang, L. Xie, J. Zheng, Y. Liu, X. Li, Superior hydrogen absorption and desorption behavior of Mg thin films, J. Power Sources 186 (2009) 515–520.
[21] R. Arndt, B. Andreas, Thin-film metal hydrides, ChemPhysChem 9 (2008) 2440–2455.
[22] K. Sushant, P. Theodore, S. Vidyadhar, N. Hoa, S. Stephan, P. Christopher, C. Bruce, K. Joseph, G. Panagiotis, S. Mukhles, Hydrogen flux through size selected Pd nanoparticles into underlying Mg nanofilms, Adv. Energy Mater. 8 (2018) 1701326.
[23] G. Liang, J. Huot, S. Boily, A. Van Neste, R. Schulz, Catalytic effect of transition metals on hydrogen sorption in nanocrystalline ball milled MgH_2–tm (tm = Ti, V, Mn, Fe and Ni) systems, J. Alloys Compd. 292 (1999) 247–252.
[24] O. Friedrichs, F. Aguey-Zinsou, J.R.A. Fernández, J.C. Sánchez-López, A. Justo, T. Klassen, R. Bormann, A. Fernández, MgH2 with Nb_2O_5 as additive, for hydrogen storage: chemical, structural and kinetic behavior with heating, Acta Mater. 54 (2006) 105–110.
[25] J. Zhang, H. Qu, G. Wu, L.B. Song, X.F. Yu, D.W. Zhou, Remarkably enhanced dehydrogenation properties and mechanisms of MgH_2 by sequential-doping of nickel and graphene, Int. J. Hydrog. Energy 41 (39) (2016) 17433–17441.
[26] X. Huang, X. Xiao, W. Zhang, X. Fan, L. Zhang, C. Cheng, S. Li, H. Ge, Q. Wang, L. Chen, Transition metal (Co, Ni) nanoparticles wrapped with carbon and their superior catalytic activities for the reversible hydrogen storage of magnesium hydride, Phys. Chem. Chem. Phys. 19 (2017) 4019–4029.
[27] J. Zhang, S. Yan, H. Qu, Recent progress in magnesium hydride modified through catalysis and nanoconfinement, Int. J. Hydrog. Energy 43 (2018) 1545–1565.
[28] L. Zhang, L. Chen, X. Fan, X. Xiao, J. Zheng, X. Huang, Enhanced hydrogen storage properties of Mgh2 with numerous hydrogen diffusion channels provided by $Na_2Ti_3O_7$ nanotubes, J. Mater. Chem. A 5 (2017) 6178–6185.
[29] L. Zhang, L. Chen, X. Xiao, X. Fan, J. Shao, S. Li, H. Ge, Q. Wang, Fluorographene nanosheets enhanced hydrogen absorption and desorption performances of magnesium hydride, Int. J. Hydrog. Energy 39 (2014) 12715–12726.
[30] Y. Liu, H. Du, X. Zhang, Y. Yang, M. Gao, H. Pan, Superior catalytic activity derived from a two-dimensional Ti_3C_2 precursor towards the hydrogen storage reaction of magnesium hydride, Chem. Commun. 52 (2016) 705–708.
[31] H. Kobayashi, M. Yamaguchi, T. Ito, Ab initio MO study on adsorption of a hydrogen molecule onto magnesium oxide (100) surface, J. Phys. Chem. 94 (1990) 7206–7213.
[32] G. Wu, J. Zhang, Y. Wu, Q. Li, K. Chou, X. Bao, Adsorption and dissociation of hydrogen on MgO surface: a first-principles study, J. Alloys Compd. 480 (2009) 788–793.
[33] E. Schröder, R. Fasel, A. Kiejna, O adsorption and incipient oxidation of the Mg (0001) surface, Phys. Rew. B 69 (2004) 115431.
[34] E. Schröder, R. Fasel, A. Kiejna, Mg(0001) surface oxidation: a two-dimensional oxide phase, Phys. Rew. B 69 (2004) 193405.
[35] M. Pozzo, D. Alfè, The role of steps in the dissociation of H_2 on Mg(0001), J. Phys. Condens. Matter 21 (2009) 095004.
[36] M. Pozzo, D. Alfè, Hydrogen dissociation and diffusion on transition metal (Ti, Zr, V, Fe, Ru, Co, Rh, Ni, Pd, Cu, Ag)-doped Mg(0001) surfaces, Int. J. Hydrog. Energy 34 (2009) 1922–1930.
[37] A.J. Du, S.C. Smith, X.D. Yao, G.Q. Lu, Hydrogen spillover mechanism on a Pd-doped mg surface as revealed by ab initio density functional calculation, J. Am. Chem. Soc. 129 (2007) 10201–10204.
[38] N. Jacobson, B. Tegner, E. Schröder, P. Hyldgaard, B.I. Lundqvist, Hydrogen dynamics in magnesium and graphite, Comput. Mater. Sci. 24 (2002) 273–277.
[39] J. Xin, J. Wang, Y. Du, L. Sun, B. Huang, Site preference and diffusion of hydrogen during hydrogenation of Mg: a first-principles study, Int. J. Hydrog. Energy 41 (2016) 3508–3516.
[40] G. Kresse, J. Furthmüller, Efficient iterative schemes for ab initio total-energy calculations using a plane-wave basis set, Phys. Rev. B 54 (1996) 11169.
[41] P.E. Blöchl, Projector augmented-wave method, Phys. Rev. B 50 (1994) 17953.
[42] J.P. Perdew, K. Burke, M. Ernzerhof, Generalized gradient approximation made simple, Phys. Rev. Lett. 77 (1996) 3865–3868.
[43] J.P. Perdew, K. Burke, Y. Wang, Generalized gradient approximation for the exchange-correlation hole of a many-electron system, Phys. Rev. B 54 (1996) 16533–16539.
[44] H.J. Monkhorst, J.D. Pack, Special points for Brillouin-zone integrations, Phys. Rev. B 13 (1976) 5188–5192.
[45] G. Henkelman, B.P. Uberuaga, H. Jónsson, A climbing image nudged elastic band method for finding saddle points and minimum energy paths, J. Chem. Phys. 113 (2000) 9901–9904.
[46] H. Lei, C. Wang, Y. Yao, Y. Wang, M. Hupalo, D. McDougall, M. Tringides, K. Ho, Strain effect on the adsorption, diffusion, and molecular dissociation of hydrogen on Mg (0001) surface, J. Chem. Phys. 139 (2013) 224702–224708.